PHILOSOPHICAL TRANSACTIONS OF THE ROYAL SOCIETY B BIOLOGICAL SCIENCES

Application of Stochastic Geometry to Problems in Plankton Ecology

B. J. Rothschild

Phil. Trans. R. Soc. Lond. B 1992 **336**, 225-237
doi: 10.1098/rstb.1992.0058

Application of stochastic geometry to problems in plankton ecology

B. J. ROTHSCHILD

University of Maryland, Center for Environmental and Estuarine Studies, Chesapeake Biological Laboratory, Box 38, Solomons, Maryland 20688-0038, U.S.A.

CONTENTS

SUMMARY

The most fundamental linkages in ecosystem dynamics are trophodynamic. A trophodynamic theory requires a framework based upon inter-organism or interparticle distance, a metric important in its own right, and an essential component relating trophodynamics and the kinetic environment. It is typically assumed that interparticle distances are drawn from a random distribution, even though particles are known to be distributed in patches. Both random and patch-structure interparticle distance are analysed using the theory of stochastic geometry. Aspects of stochastic geometry – point processes and random closed sets (RCS) – useful for studying plankton ecology are presented. For point-process theory, the interparticle distances, random-distribution order statistics, transitions from random to patch structures, and second-order-moment functions are described. For RCS-theory, the volume fractions, contact distributions, and covariance functions are given. Applications of stochastic-geometry theory relate to nutrient flux among organisms, grazing, and coupling between turbulent flow and biological processes. The theory shows that particles are statistically closer than implied by the literature, substantially resolving the troublesome issues of autotroph–heterotroph nutrient exchange; that the microzone notion can be extended by RCS; that patch structure can substantially modify predator–prey encounter rates, even though the number of prey is fixed; and that interparticle distances and the RCS covariance function provide a fundamental coupling with physical processes. In addition to contributing to the understanding of plankton ecology, stochastic geometry is a potentially useful for improving the design of acoustic and optical sensors.

1. INTRODUCTION

Understanding variability in community metabolism (Allee *et al.* 1949, p. 495) of the upper ocean (Longhurst & Harrison 1989; Jahnke 1990) is important to assessing effects of global change, anthropogenic substances, and resource exploitation. The study of upper-ocean community metabolism is usually accomplished by aggregating taxonomic groups (e.g. phytoplankton, zooplankton, etc.) and then accounting for inputs and outputs of carbon (or other material).

The aggregative approach presents a dilemma. On one hand, aggregation obscures the density-dependent, population-regulation mechanisms of each population which are critical to understanding community-metabolism variability. On the other hand, the study of each individual population's density-dependent, population-regulation phenomena is impractical.

One resolution of this dilemma involves focusing on how the ecosystem functions, rather than on a description of the relationships among taxonomic assem-

Phil. Trans. R. Soc. Lond. B (1992) **336,** 225–237
Printed in Great Britain

blages. A major component of ecosystem function involves the integration of trophodynamics by population dynamics and the integration of population dynamics by community metabolism (see Rothschild 1986, pp. 218–236). The integrations imply that major sources of community-metabolism variability are driven by trophodynamic interactions. Although trophodynamic interactions are fundamental and important in their own right, they also provide the basic connection between population dynamics and the kinetic physical environment (Rothschild & Osborn 1988). These trophodynamic interactions provide a universal linkage among the populations in the ocean ecosystem or community, as the interactions can be thought of in the conventional sense of carnivory, and also in the sense that grazers 'predate' upon phytoplankton cells; phytoplankton cells 'predate' upon photons and nutrient molecules; and small heterotrophs 'predate' upon nutrient molecules.

An analysis of trophodynamics can be initiated from a consideration of the classical population-dynamics theory. In this theory, the interaction between predator and prey is often thought of as some function (see Holling 1965) of the product of predator-and-prey abundance (i.e. $f(N_1N_2)$, where N_1 is the abundance of prey, and N_2 is abundance of predators). The assumptions that (i) predator and prey are distributed randomly, and (ii) that predator–prey encounter is independent of their relative velocity are implicit in the classic formulation.

These assumptions of the classical approach are only partially addressed in the literature. The factors related to relative motion (Gerritsen & Strickler 1977), turbulent-flow enhanced relative motion (Rothschild & Osborn 1988), and 'diffusion' (Davis *et al.* 1991) are now well known. In contrast, although the issues of patch structure have been known since the 1950s (e.g. Cassie 1959), there have been only a few serious studies of the structure of patchiness (see, for example, Fasham 1978*a*, *b*). If the predator and prey are in patches, rather than randomly distributed, the immediate effects of motion on the encounter of predator and prey will be different. The existence of a patch structure means that the theory of the interactions among predator-and-prey organisms related to relative motion and turbulent flow needs to be extended to account for non-random distribution or patch structure.

Extension of theory to account for patch structure requires, as a first step, the description of a physical framework for the distribution of predator-and-prey 'particles' in Euclidean space. A physical framework enables (i) calculations of interparticle distance, a statistic involving the propensity for trophodynamic interaction; (ii) definition and comparison of various patch structures; and (iii) specification of initial conditions for studying effects of the physical environment, such as fluid flow, on particle distribution.

A physical framework for the probability distribution of particles in space or interparticle distances is covered by the theory of stochastic geometry (see the basic text by Stoyan *et al.* (1987); most of the theory is reported or derived from their results). This paper brings together aspects of the theory of stochastic geometry that pertain to applications in plankton ecology. The theory involves both point processes and random closed sets (RCS). The theoretical results illustrate the application of point-process theory and the potential of RCS theory to plankton ecology.

The first part of the paper articulates necessary aspects of the theory of stochastic geometry. Specifically for point-process theory, the statistical distribution of interparticle distances, random-distribution order statistics, the transition between random and patch structure, and second-order moments are presented. For RCS theory, the basic summarization statistics are given explicitly for the Boolean model along with the notions of patch coalescence and the integral feeding scale.

In the second part of the paper, applications of stochastic geometry to plankton ecology are considered. In particular, the theory is applied to the question of rates of nutrient flux as a function of interparticle distance and the potential effects of prey distribution on grazing. With regard to nutrient flux, the theory indicates many interparticle distances are smaller than those deduced from the deterministic calculations presented in the literature, suggesting that nutrients are exchanged at higher than diffuse background-level rates. RCS calculations of 'spheres-of-influence' explore expectations of nutrient exchange relative to microzones of algal cells to further extend these conclusions. Application of stochastic geometry to prey-patch structure illustrates how patch structure can affect rates of predator–prey interaction even though the number of prey is constant. For point processes, the transition from a random distribution to a patchy distribution of phytoplankton is demonstrated. For RCS, volume fractions of prey patches, their contact distributions and the covariance function of interparticle distances within and between patches are used to define probable levels of interaction at varying patch density and size. The concept of a feeding length scale is used to define distances of prey from a predator.

The third part of the paper illustrates the role of stochastic geometry in the coupling between trophodynamics and physical forcing and sets the stage for deriving the statistical distribution of turbulence-induced particle velocity for non-random statistical distributions of particles.

2. STOCHASTIC GEOMETRY

The study of the particulate foundations of community-metabolism variability begins by considering the living or otherwise bioactive particles of the upper ocean as a set of spatially stochastic points. Each point is a locus of biodynamic transformation: phytoplankton cells transform photons and nutrient molecules into biomass, copepods 'destroy' and then convert phytoplankton cells into copepod biomass, catabolites, pellets, etc.

The intensity of the transformational process is driven by trophic transactions of particle–particle interactions. In turn, the intensity of particle–particle

interaction is a function of interparticle distance. Interparticle distance is a function of particle distribution. Particle distribution and the metabolic function partition $N(n)$, can be written

$$\Psi = \{X_i; \delta_j(X_i)\}, \qquad N(n) = \sum_{j=1}^{m} n_j = N, \tag{1}$$

where X_i is the three-dimensional stochastic position of the $i = 1, \ldots, N$ particles, $\delta_j(X_i)$ is the jth metabolic function $j = 1, \ldots, M$ of the ith particle, and n_j is the number of particles having the jth metabolic function.

There are many possible classifications of δ_j. These classifications can be specific for taxa, size, location, etc. One simplified classification of metabolic function might be $j = 1$, micro-autotroph; $j = 2$, micro-heterotroph; $j = 3$, large autotroph; $j = 4$, large grazer; $j = 5$, predator.

The geometry implied by equation (1) can be studies via both point-process and RCS theory. Section 1 elaborates upon the theory of random distributions, § 2 describes patch structure in terms of the mixed Poisson-point process and § 3 outlines essential elements of RCS theory.

(*a*) *The random model*

The random or Poisson probability distribution implies that the probability distribution function of the distance to the nearest neighbour (see, for example, Pielou 1977) is

$$D_R(r) = 1 - \exp(-\tfrac{4}{3}\lambda\pi r^3), \tag{2}$$

where λ is the mean density of particles in three-dimensional space and r is the nearest-neighbour distance between particles. The derivative of equation (2) yields the probability density function

$$D'_R(r) = 4\lambda\pi r^2 \exp(-\tfrac{4}{3}\lambda\pi r^3), \tag{3}$$

which enables calculation of the mean nearest-neighbour distance (NND):

$$\bar{r} = 4\lambda\pi \int_0^\infty r^3 \exp(-\tfrac{4}{3}\lambda\pi r^3)\, \mathrm{d}r. \tag{4}$$

Integration of equation (4)† yields the NND

$$\bar{r} = 0.55\lambda^{-\frac{1}{3}}. \tag{5}$$

It is important to recognize that $\bar{r}$, is an average value. This means that when $\bar{r}$ is used to appraise interactions among particles, roughly half of the interactions will be based upon distances that are less than $\bar{r}$, and half the interactions will be based on distances greater than $\bar{r}$.

Distances other than the mean distance are important. As an example, consider the minimum mean distance to the nearest neighbour, MNND. The theory of order statistics is used to compute the MNND. N independent NNDs are measured and ranked from smallest to largest to obtain $R_1, R_2, \ldots, R_N$. Instead of $\bar{r}$, the mean distance to the nearest neighbour, we are now interested in $\bar{r}^*$, the mean minimum distance to the nearest neighbour. The mean of the minimum of all R_i observations, R_1 (as distinct from the distribution of the random variable R) is obtained from the general formula for the probability density function for the minimum value of order statistics

$$D_R(r_1) = n[1 - D_R(r)]^{n-1} D'_R(r), \tag{6}$$

using equation (2) and equation (3) in equation (6) we have

$$D_R(r_1) = 4n\lambda\pi r_2 \exp(-\tfrac{4}{3}n\lambda\pi r^3). \tag{7}$$

Calculating the mean from equation (7)

$$\bar{r}^* = n4\lambda\pi \int_0^\infty r^3 \exp(-\tfrac{4}{3}n\lambda\pi r^3)\mathrm{d}r. \tag{8}$$

The integral of equation (8) is

$$\bar{r}^* = 0.55\, n^{-\frac{1}{3}} \lambda^{-\frac{1}{3}}. \tag{9}$$

In other words, as n increases, the mean MNND decreases. We are led to the conclusion that if we are interested in average distances then $\bar{r}$ is the appropriate statistic, but if we are interested in how close distances might be, given n, then $\bar{r}^*$ is appropriate. Inasmuch as there are always very many particles, and many independent distances, some interparticle distances can be made to be arbitrarily small.

(*b*) *Patch models*

There are several classes of patch-structure models (see, for example, Fasham 1978*a*, *b*). It has been shown, however, that empirical data on spatial distribution alone are not sufficient to identify underlying patch-structuring mechanisms (Pielou 1977). The alternative, identifying a class of patch-structure models based on first principles is equally problematic, because the first principles are not yet well understood. Nevertheless, much of the flavour of the patch-structure problem can be gleaned from simple examples. As an example, consider two different classes of patch models, a point-process mixed-Poisson model and a RCS model. These examples enable qualitative appraisal of the nature of patchiness, pending a more detailed study of mechanisms.

(i) *The transition from random to patch structure*

The mixed Poisson distribution is a patch-structure model containing as a special case, the random, non-patch structure, Poisson distribution. The mixed-Poisson distribution is a mixture of a low-density Poisson parameter λ_1 and a high-density Poisson parameter, λ_2 (i.e. $\lambda_1 < \lambda_2$). Thus λ_2 can be thought of as an intrapatch density whereas λ_1 can be thought of as an interpatch density. Thus the mixed-Poisson distribution does not generate patches per se but rather point-wise, independent, high and low densities. The mixing parameter is υ so λ_1 is specified to occur with probability $(1 - \upsilon)$ and λ_2 with probability υ (for a detailed analysis of this process in connection with the biological functional response, see Rothschild (1991)). The random special case is obtained by

† Integration of equation (4) and equation (8) involves integration of a gamma function. Solutions are not available in simple tables. The appropriate formula is

$$\int_0^\infty x^m \mathrm{e}^{-ax^n}\, \mathrm{d}x = (1/na^{(m+1)/n})\Gamma[(m+1)/n].$$

PHILOSOPHICAL TRANSACTIONS OF THE ROYAL SOCIETY B BIOLOGICAL SCIENCES

setting $\lambda_1 = \lambda_2$. Also, as v approaches zero or 1, the mixed-Poisson distribution approaches the random or Poisson distribution.

The mean of the process is

$$\bar{\lambda} = (1 - v)\lambda_1 + v\lambda_2. \tag{10}$$

The NND distribution function is

$$D(r) = \bar{\lambda}^{-1}[\lambda_1 (1 - v)(1 - e^{-\lambda_1 \omega r^3}) + \lambda_2 v(1 - e^{-\lambda_2 \omega r^3})], \tag{11}$$

where $\omega = \frac{4}{3}\pi$. The probability density function derived from equation (11), is

$$D'(r) = 3\alpha\lambda_1 \omega r^2 e^{-\lambda_1 \omega r^3} + 3\beta\lambda_2 \omega r^2 e^{-\lambda_2 \omega r^3}, \quad \alpha = \bar{\lambda}^{-1}\lambda_1(1 - v), \quad \beta = \bar{\lambda}^{-1}\lambda_2 v. \tag{12}$$

Accordingly the mean NND is

$$\bar{r} = 3\omega \int_0^\infty [\alpha\lambda_1 r^3 e^{-\lambda_1 \omega r^3} + \beta\lambda_2 r^3 e^{-\lambda_2 \omega r^3}]dr, = 0.55\bar{\lambda}^{-1}[(1 - v)\lambda_1^{2/3} + v\lambda_2^{2/3}]. \tag{13}$$

The reduced-second-order moment function (RSOMF) or the ratio between the number of particles a distance less than r and the overall mean-density $\bar{\lambda}$ is

$$K(r) = \left[\frac{\lambda_1^2 (1 - v) + \lambda_2^2 v}{\lambda_1 (1 - v) + \lambda_2 v}\right][\tfrac{4}{3}\pi r]. \tag{14}$$

Put another way, the product of the mean density $\bar{\lambda}$ and the RSOMF gives the expected number of particles, a distance less than r.

If distributions are Poisson or random, then all of the information on the distribution is contained in the first moment or the mean in the sense that the mean and variance are equal. If, however, distributions are patchy, then the second-order properties of the distribution need to be considered. To emphasize this point, consider that in a patchy distribution, in contrast to a random distribution, knowing the overall mean, $\bar{\lambda}$, does not imply unique value for $\bar{r}$, the NND.

(ii) *Random closed sets (RCS)*

The theory of random closed sets can be used to take a different approach to spatial-patch distribution.

A RCS is defined as

$$\Xi = (\Xi_1 + x_1) \cup (\Xi_2 + x_2) \cup \ldots \cup (\Xi_N + x_N), \tag{15}$$

where x_i is the position in 3-dimensional Euclidean space of the ith RCS and Ξ_i is the RCS associated with x_i. The x_is are called the 'germs' of the process while a typical Ξ_i, Ξ_0 is called a 'primary grain' (note that Ξ_0 is not one of the Ξ_is). If $\phi = \{x_1, x_2, \ldots\}$ is a statistically stationary Poisson process and if the primary grains can be considered as closed sets, then Ξ is called a Boolean model. The first and second-order properties of the Boolean model are well known.

For our applications of RCS theory we consider the primary grain to be a sphere with radius r. The radius of the sphere is taken as a random variable. We might think of each random sphere as a collection of particles enclosed by the sphere perimeter. The particles inside the spheres have equal density, or some minimum density, or densities which are functions of the sphere radius. The spheres can be thought of as 'spheres of influence'.

Given that the germs are randomly distributed with intensity λ and that the primary grain is a sphere with normally distributed radius $N(\mu,\sigma^2)$, and hence third moment, $3\mu\sigma^2 + \mu^3$, we can examine (i) the volume fraction; (ii) the parameter of the chord length distribution; (iii) the contact distribution, and (iv) the covariance function. We observe here that the normal distribution is used for heuristic purposes, technically having no lower bound, its replacement by a gamma distribution (for example) would be more rigorous. In addition, very large variances mimicking larger-scale and more complex patch structure could be more comfortably accommodated with the gamma distribution.

The volume fraction of the percentage of the volume occupied by Ξ with the parameter set $\Xi(\lambda,\mu,\sigma^2)$ is

$$p = 1 - \exp(-\tfrac{4}{3}\lambda\pi(3\mu\sigma^2 + \mu^3)), \tag{16}$$

where λ is the intensity of the 'germs' and $(3\mu\sigma^2 + \mu^3)$ is the third moment associated with the normally distributed radius of the primary grain. Inspection of equation (16) reveals that an increase in any of the parameters increases the volume fraction.

The volume-fraction statistic p requires careful interpretation. When p is small there is only a small chance of overlap in the primary grains. However, as p becomes large the chance of overlap increases. So the Boolean model really represents two patch modalities: (i) for small p, the patchiness results from confining particles to spheres; (ii) for large p, patchiness is complex in the sense that patchiness results from confining particles to spheres and from the intersection of spheres where the densities of particles are at least doubled.

A 'mean free' path among the spheres can be deduced. The chord lengths between spheres is exponentially distributed with parameter

$$L = \lambda\pi\mu. \tag{17}$$

This is the parameter of the familiar waiting-time distribution and enables modeling interactions among the particles as a stochastic process. In particular equation (17) has important applications in reduced-dimensionality problems. One example involves a large phytoplankton cell sinking through a three-dimensional volume. Another involves the penetration of a light beam through the volume (having applicability *in situ* or in remote sensing).

The spherical contact distribution is given as

$$H(r) = 1 - \exp(-\lambda\pi r(4(\sigma^2 + \mu^2) + 4\mu r + \tfrac{4}{3}r^2)). \tag{18}$$

This is the distance to the nearest sphere from a randomly chosen point outside a sphere. Accordingly $H(r)$ gives a measure of one-dimensional 'void space' from a randomly selected three-dimensional vantage point, not in a sphere of influence.

Finally, the covariance function specifies the distri-

PHILOSOPHICAL TRANSACTIONS OF THE ROYAL SOCIETY B BIOLOGICAL SCIENCES

bution of distances between points (as distinct from germs) within and among spheres.

$$C(r = 2p - 1 + (1 - p)^2 \exp\left[\tfrac{4}{3}\lambda\pi \int_{r/2}^{\infty} x^3 \left(1 - \frac{3r}{4x} + \frac{r^3}{16x^3}\right) \mathrm{d}F_r(x)\right], \quad (19)$$

where

$$\mathrm{d}F_r(x) = (1/\sigma\sqrt{2\pi})\exp - [(x-\mu)^2/2\sigma^2], \quad (20)$$

because r is $N(\mu,\sigma^2)$.

The covariance function characterizes the spacing among germs and primary grains. Note that the maximum value of the covariance function is p and the minimum value is asymptotically p^2. In a sense the covariance measures the rapidity with respect to r that the covariance declines.

The covariance function can be used to define an integral feeding scale

$$\mathscr{F} = \int_0^{\infty} C(r)\mathrm{d}r. \quad (21)$$

The scale $\mathscr{F}$ might be perceived by a predator feeding among prey with specified germ and typical grain distributions. $\mathscr{F}$ is a natural coupling with feeding biology in the context of the theory of homogenous and isotropic turbulence.

The theory of random closed sets easily lends itself to considering certain aspects of the intersections among RCS. For example, consider the joint volume fractions and covariance functions

$$P = \prod_{i=1}^{N} p_i, \qquad C(r) = \prod_{i=1}^{N} C_i(r). \quad (22)$$

When $N=2$; $i=1$ could refer to a predator; and $i=2$, to a prey. Larger N could represent various scales of patchiness. Formulations such as equation (22) permit considerable flexibility.

3. APPLICATIONS TO PLANKTON ECOLOGY

This section gives applications of stochastic geometry to the study of plankton ecology, particularly the molecular-nutrient flux and grazing. Use of actual data in developing applications is difficult because (i) knowledge of physiological anabolic–catabolic microplankton kinetics is limited; (ii) most reports pertinent to particel–particle interactions are based on a variety of inconsistent units and measurement approaches (e.g. units of carbon, parts-per-million of particles, chlorophyll, numbers of prey-per-unit-volume, and behavioral responses), rather than actual particle counts; and finally (iii) in rare cases where particle counts are given, only first-order properties are reported.

(*a*) *Rates of inter-organism nutrient flux*

Rates of nutrient flux among organisms are a function of the diffusive properties of nutrient molecules and the distance between donor and acceptor cells (or donor organisms and acceptor cells). The interparticle distance can be studied in terms of point processes and RCS. The first example, using point processes shows that contrary to the literature, many particles are statistically much closer to one another than reported. This is because the reported distances are based upon mean distances; the mean distance both under- and over-estimate the actual distance of most particles. A very large number of particles are at distances less than the mean distance. The close proximity of donors and acceptors implies a commonplace nutrient exchange between donor and acceptor cells at greater than diffuse background levels. Stochastic geometry is used to make precise the notion of the probability distribution of interparticle distance. The second example uses RCS to develop a geometric foundation for the study of microzones or relatively high concentrations of nutrients surrounding a nutrient donor.

(i) *The proximity of particles and point-theory process*

An outstanding problem in the study of molecular-nutrient flux is the rate of transfer of nutrient molecules from donors to acceptors (nutrient donors range in size from microbial to the largest organisms: nutrient acceptors are autotrophs, 1–50 μm and heterotrophs, less than 5 μm). This problem (originally configured in terms of 'large' donors and 'small' acceptors) was recently reviewed (Jackson 1987; Mann & Lazier 1991; see also, Goldman 1988, Le Fèvre & Frontier 1988). There are two contradictory, and unresolved points of view. The first point of view is that nutrient exchange occurs at a high rate to sustain observed production. The second point of view is that the mean distance between donor and acceptor particles is so 'large' that, nutrients reach a diffuse background level before they can be exchanged at a relatively high flux rate.

The interpretive difficulty arises because the distances between cells reported in the literature are essentially deterministic (and, in some instances, incorrect mathematically). However, because the actual distance between cells is a chance variable, it can be shown that many cells are much closer to one another than the deterministic distance. So on a conservative geometric basis the transfer of nutrients at relative high rates appears quite plausible.

To see this, consider the spatial distribution of picoplankton relative to a random point occupied by an autotroph. Assuming that there are 1.5×10^6 picoplankton per cubic centimetre; that each picoplankton has a radius of 1 μm; and that the autotroph has a radius of 10 μm, the NND among the picoplankton is 48 μm. This random mean distance is conservative (under patch structure, the particle would be even closer (cf. equations 5 and 13)).

This means that the average distance between cell walls is 37 μm. The probability distribution function corresponding to these specifications is shown in figure 1. Roughly half the pico-plankton cells are within 37 μm of the autotroph cell wall. Taking expectations, $p = 0.06\%$ of the nearest-neighbour distances are so close as 10 μm distant from the autotroph. This amounts to 90000 nearest-neighbour distances. Examination of the RSOMF shows that on the average

PHILOSOPHICAL TRANSACTIONS OF THE ROYAL SOCIETY B BIOLOGICAL SCIENCES

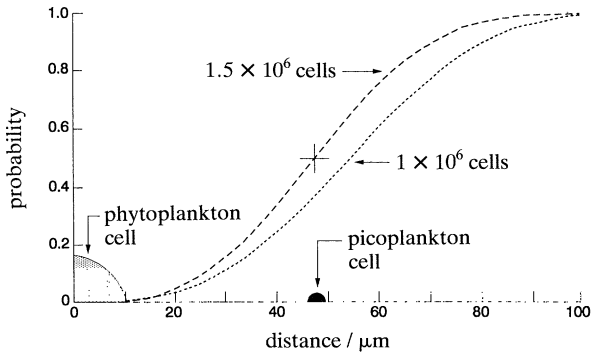

Figure 1. Probability distribution function for NND given a Poisson distribution and cell densities of 1×10^6 and 1.5×10^6 cells per cubic centimetre. A phytoplankton cell and a picoplanktonic heterotroph are superimposed at what might be a typical distance. The cross marks the mean NND for 1.5×10^6 random particle distance.

six cells are in a shell having inside diameter of about 50 μm and an outside diameter of about 100 μm (figure 2). This is of interest because while on one hand there are on the average six cells within 100 μm of a typical cell, there are on average no cells within 50 μm. It is reasonable to expect that, of these, half will be closer than the NND to each other and hence could increase the local density of catabolites. On consideration of the probability distribution of NND and the MNND in the random case, it is likely that at any fixed instant some autotrophs and heterotrophs are sufficiently close to exchange or transmit metabolites at concentrations in excess of background levels, a line of reasoning further certified by the MNND calculation.

These results apply mostly to pico- and microplankton nutrient exchange, but what about large heterotroph donors (e.g. copepods)? To consider this situation, we observe that the major groups of plankton can be classified by size and density (i.e. numbers per unit volume). For example, large zooplankton are about 1000 μm in diameter and occur at densities of 10^{-2} individuals per cubic centimetre. Large phytoplankton are of the order of 100 μm in diameter and occur at densities of 100 individuals per cubic centimeter. Picoplankton are about 1 μm in diameter and occur at densities of 10^6 individuals per cubic centimetre.

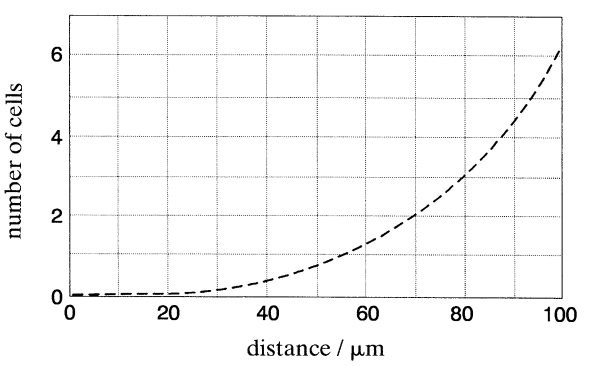

Figure 2. The product of the mean density and the RSOMF for a Poisson distribution with mean density 1.5×10^6 cells per cubic centimetre. The RSOMF gives the mean number of cells within distance r from a particle. There are roughly six cells in a spherical shell between 50 and 100 μm.

The densities enable computing the NND (equation 5) and MNND (equation 9) for each major group. These are plotted in figure 3. It will be noted that picoplankton have an interparticle distance of only roughly 10^{-3} cm, whereas the diameter of a large zooplankton is about 10^{-1} cm. Therefore the large zooplankton and picoplankton are in 'continual contact' (see also Rothschild 1988).

The proximity of large zooplankton and picoplankton raises two points. The first is that the relatively large size of the zooplankton and the relatively small interparticle distance of the picoplankton suggests that large zooplankton could contribute nutrients to picoplankton at rates higher than might otherwise be thought. In addition, the fact that zooplankton grazers are often in very close proximity (because the zooplankton graze on the autotrophs) to larger autotrophs implies that large zooplankton donate molecular nutrients to larger autotrophs as well.

The entire transfer process would be even more efficient if the zooplankton had an efficient way of finding the phytoplankton patches. This raises the second point which is the speculation that catabolizing picoplankton provide directional guidance for grazing zooplankton, even though the picoplankton are too small to be ingested by larger zooplankton. The basic idea is that phytoplankton exudates are metabolized by picoplankton and that picoplankton catabolites provide a more efficient directional sense to chemotactic zooplankton regarding their orientation toward phytoplankton patches. The phytoplankton 'leak' organic molecules, the molecules are 'ingested', then catabolized by picoplankton, and finally the diffused picoplankton catabolites are detected at relatively high concentrations by grazer chemoreceptors, which are almost in direct contact with the picoplankton cells. In other words the picoplankton serve as chemical 'repeaters' (much as in a radio transmission system) and enable detection of the presence and

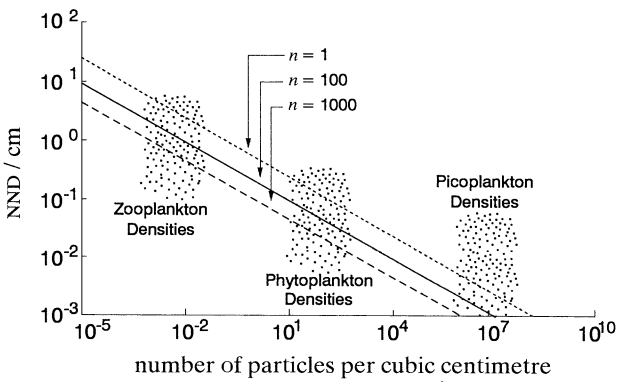

Figure 3. Nearest neighbor distance (NND) as a function of particle density. The line corresponding to $n = 1$ is the conventional NND. The lines corresponding to $n = 100$ and $n = 1000$ are MNNDs for $n = 100$ and $n = 1000$ respectively. Typical ranges of numerical densities (which generally do not overlap) are shown for zooplankton, phytoplankton, and picoplankton.

PHILOSOPHICAL TRANSACTIONS OF THE ROYAL SOCIETY B BIOLOGICAL SCIENCES

direction of a phytoplankton patch at a greater range than if the grazers were using only the phytoplankton exudates for chemotactic spatial clues. The operation of this scenario requires chemical signals at different intensities at closely spaced chemoreceptors. If the scenario were operable under certain conditions, the trophodynamic coupling among different size groups of plankton would be much greater than otherwise thought.

(ii) *Microzones and* RCS *theory*

RCS theory can be specifically applied to the molecular-nutrient, 'sphere-of-influence', or microzone (Mitchell *et al.* 1985) around each particle. Mitchell *et al.* give the radius of a microzone,

$$r = Q/4\pi DC' \qquad (23)$$

where Q is the total nutrient flux per cell, D is the molecular diffusivity and C is threshold concentration (they set $C=0.10$) above background concentration. Using this formula, they compute that the algal-cell DOC microzone, 10% above background level, would have a radius of *ca.* 1 mm.

As Mitchell *et al.* imply, assessments of microzone dimensions are uncertain. In particular, there are many alternative assumptions regarding the factors that drive the temporal and spatial microzone volume. These include the temporal relation between anabolite and catabolite; input–output, and donor volume, versus donor surface-area per unit cell volume.

Because the magnitude of the microzone radius (both temporally and spatially) is uncertain, it can be treated as a variable enabling the study of the volume fraction as a function of microzone radius. The volume fraction occupied by the spheres-of-influence of the large autotrophs (based on a density of 400 individuals per cubic centimetre is plotted in figure 4). If we agree that a microzone radius of 100 μm is 'large', then we see that even at this large volume only 2.5×10^{-4} of the volume is occupied by large autotroph microzones. On the other hand, there are a very large number of small heterotrophs, so at a large microzone radius of 100 μm and a concentration of 1.5×10^6 heterotroph cells per cubic centimetre, we would expect to find $(1.5 \times 10^6) \cdot (2.5 \times 10^{-4}) = 3.75 \times 10^2$ small heterotrophs per cubic centimetre within autotroph microzones.

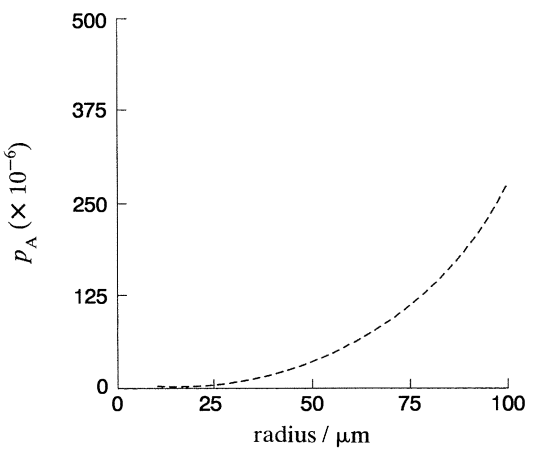

Figure 4. Relation between volume fraction, p_A, and radius of sphere of influence for autotroph where $\lambda_A = 400\ \mathrm{cm}^{-3}$, and $\sigma_A^2 = \frac{1}{4}\mu^2$.

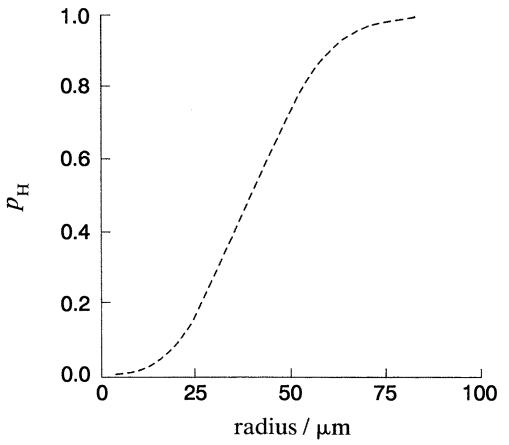

Figure 5. Relation between volume fraction p_H and radius of sphere of influence for heterotroph, where $\lambda_H = 1.5 \times 10^6$, and $\sigma_H^2 = \frac{1}{4}\mu^2$.

The volume fraction p_h and the radius of the sphere of influence for a small heterotroph (having a density of $1.5 \times 10^6\ \mathrm{cm}^{-3}$) is plotted in figure 5. By contrast the volume fraction increases much more rapidly by virtue of the fact that the numerical density of small heterotrophs is much greater than that of large autotrophs. Placing a large autotroph in a field of small heterotrophs leads to the statistical expectation that interactions at higher than background levels would be expected.

The notion of the volume fraction can be used to estimate the volume of zones of synergy or 'hot spots' between particles. To give an example of these calculations to estimate the intersection of microzones the pool of picoplankton is divided into two groups of 0.75×10^6 cells per cubic centimetre each. The effect of the radius of the sphere of influence on the volume of intersection of spheres can be calculated using equation (22). The results of the calculations are shown in figure 6. The figure shows that the length of the radius has to be at least 20 μm before interaction occurs. Between a radius of 20 μm and a radius of 50 μm, roughly from 40–100% of the average NND, the

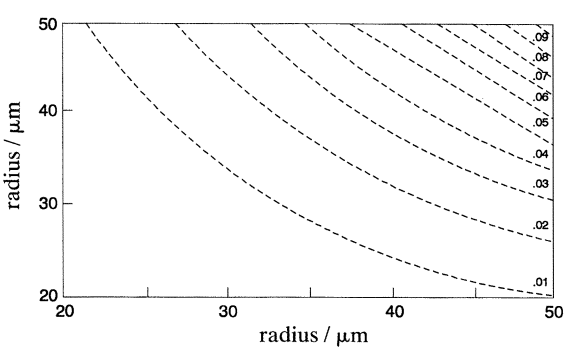

Figure 6. Volume fraction occupied by overlapping spheres of influence from two populations, each 0.75×10^6 cells per cubic centimetre and with specified radius.

PHILOSOPHICAL TRANSACTIONS OF THE ROYAL SOCIETY B BIOLOGICAL SCIENCES

volume occupied by catabolites from the two pools of cells taken jointly increases from 0–10%. The overlaps would increase if the radii were considered to have a variance. The crucial question regarding joint 'hot spots' is whether conditions exist such microzones have radii greater than 20 μm. On the other hand such 'hot spots' almost certainly exist given the arguments implied by equation (9), that is MNND for various n become important.

(*b*) *Grazing: the structure of phytoplankton patchiness*

The dynamics of grazers and the phytoplankton cells upon which they feed depends to a considerable extent upon grazer–phytoplankton-cell encounter rates (Gerritsen & Strickler 1977). The study of encounter rates has generally assumed implicitly that prey are distributed at random relative to the predator. However, because plankton are generally distributed in a patch structure, the randomness assumption generates a misleading view of grazer-phytoplankton trophodynamics.

To explore the effect of patch structure on grazer–phytoplankton interactions, point-process theory can be used to consider the transition from a random distribution to patch structure. RCS theory can be used to demonstrate an alternative to point-process theory for the study of patch structure. Both branches of theory are used to show that a fixed number or density of phytoplankton cells can be allocated in space in a variety of ways and that each allocation has different consequences for the grazing and phytoplankton populations. In other words the information regarding spatial allocation can be as critical as the actual abundance of phytoplankton cells.

This is a point not generally recognized in the literature. Results of feeding experiments and observations in the field generally report only the density of zooplankton and phytoplankton. But the encounter and the number of phytoplankton cells ingested which are equally important from an ecological point of view depend to a considerable extent on the generally unreported patch structure. Furthermore, the encounter rate depends upon feeding scales rather than on anthropocentric sampling scales.

(i) *Phytoplankton patch structure: the point-process onset of patch structure*

The transition from random to patch structure occurs via the transition from equation 5 to equation 13. We suppose that phytoplankton cells have intrapatch densities (λ_2) ranging from 0–700 cells per cubic centimetre and interpatch densities (λ_1) ranging from 0–700 cells per cubic centimetre. For demonstration purposes, we select the parameter, $v = 0.75$ (as v decreases contours rotate to the vertical). The mean overall densities and the NNDs for these combinations are shown in figure 7. Let us focus on a single fixed mean density, 400 cells per cubic centimetre, for example. At the point where the intrapatch and interpatch densities are equal to 400 cells, the distribution is random or Poisson, and the NND is roughly

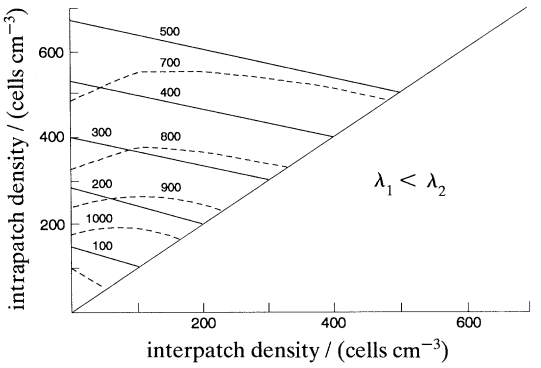

Figure 7. Contours of $\bar{\lambda}$ and NND for the mixed Poisson distribution with parameter $v = 0.75$ for various intra- and interpatch densities. Solid line, population density (cells per cubic centimetre); dashed line, nearest-neighbour density (μm).

750 μm. Transiting from a random to a patch structure and constraining observations to maintain a mean density of 400 cells per cubic centimetre the NND drops to about 700 μm at intrapatch densities of slightly more than 500 cells per cubic centimetre and interpatch densities of roughly 50 cells per cubic centimetre. The importance of this reduction in NND needs further study. However, from a copepod's point of view, traveling at 720 cm h^{-1}, it means that it would increase its encounter rate on the average, from about 9600 to 1029 cells per hour. Examining now the same 400 cell population isoline in connection with the RSOMF (figure 8) shows that the RSOMF constant parameter increases from 400 to 500 as patchiness increases over the same range of intra- and interpatch densities. The effect of increasing the RSOMF constant is shown in figure 9. This shows that in a 720 cm search sphere the random and patchy distribution would yield populations of roughly 3×10^7 and 4×10^7 cells respectively. In other words, particle patch structure has increased the opportunity of contact in a fixed radius of 720 cm search sphere by 33% bringing to mind the question of random versus directed search on the part of the copepod: for the copepod to really take advantage of the increased numbers of cells in a patch

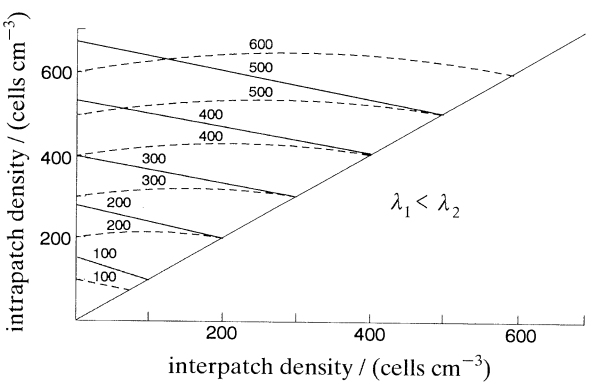

Figure 8. Contours of $\bar{\lambda}$ and the RSOMF with parameter $v = 0.75$ for various intra and interpatch densities. Solid line, populations density (cells per cubic centimetre); dashed line, parameter value.

PHILOSOPHICAL TRANSACTIONS OF THE ROYAL SOCIETY B BIOLOGICAL SCIENCES

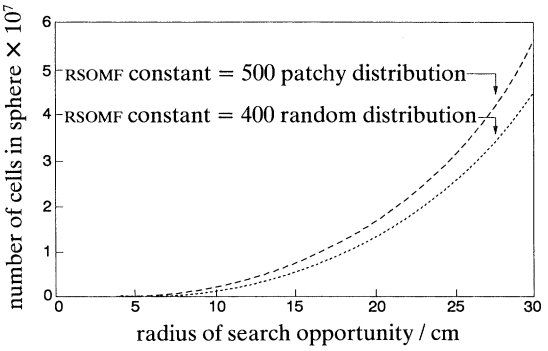

Figure 9. Product mean density and RSOMF showing the increase in feeding opportunities per unit radius of search sphere.

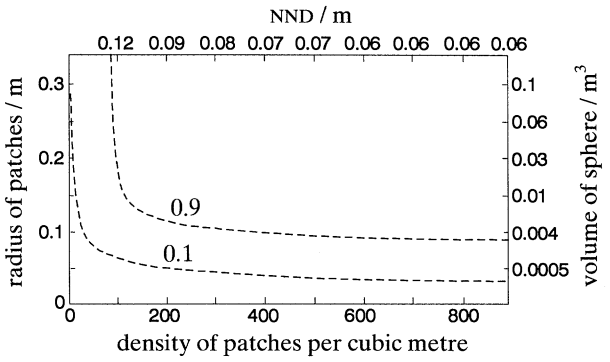

Figure 10. Boolean model, volume fraction as a function of patch radius or volume and patch density or interpatch center NND.

environment, it would have to find situations where the nearest-neighbour distance was substantially less than, say, 700 μm.

This further brings to mind the contrast between $\bar{r}$ and $\bar{r}^*$ (equation (5) and equation (9)). To put the question more precisely, do copepods capitalize on MNNDs and if they do, then is $n > 1$ a measurable function of the physical environment?

(ii) *The* RCS *model*

The RCS view of phytoplankton patch structure accommodates different information than the point-process approach. In the point-process approach, it is necessary to specify only the nature of the process (e.g. a particular cluster process) and its parameter values. The RCS theory requires specification of the germ probability distribution, the form of the primary grain, the statistical distribution of primary grain dimensions, and the way that the plankton particles are allocated within the bounds of the primary grain. These statistics enable calculation of the volume fraction, contact distribution, covariances, integral scales, etc.

The simplest RCS patch structure is the Boolean spherical model where the germs are randomly distributed and the primary grain is a sphere with a random radius. As an example, consider figure 10 which shows the volume fraction for the Boolean spherical model as a function of patch density, and patch radius. Because of the Boolean assumption, patch density immediately gives the NND of patch centres whereas the patch volume is determined from its radius. Figure 10 shows the inter-relationships in an allocation scheme of patch density; patch radius and volume fraction. We can also see that when the volume fraction is low and the primary-grain radius is low then there is an on the average separation of spheres, but when these variables are high the spheres coalesce.

The property of grain coalescence that occurs at high volume fractions (e.g. *ca.* $p > 0.2$) and high $r^3{:}\lambda$ ratios is a particularly important research topic. This is because a volume containing some coalesced patches or grains has *ceteris paribus* a much different propensity for biodynamic transformation than a volume containing no coalescence. In a sense, the onset of coalescence is analogous to changes in deterministic systems at bifurcation points or bifurcation surfaces. The difference is that in deterministic systems, the bifurcation point or surface is fixed. By contrast, in the stochastic system, the onset of coalescence is a chance variable.

What is remarkable, is that whereas the volume fraction measures the propensity for coalescence in terms of the patches or grains, the contact distribution and the covariance function relate to the particle–particle relationships of the points within the patches or grains, whether or not one or more coalesced spheres are present. For example, given some specification of the Boolean model, the contact distribution gives an approximate (the approximation relates to the stochastic distance from random point to a particle which is a function of the density of the points within the sphere) probability distribution of distance of a random grazing copepod from the nearest patch. Or, given some randomly placed particle within a patch, the covariance function approximates the probability distribution of the distance from the particle to any other particle in the system, whether it is in the same patch, or a different patch, whether or not coalescence has occurred. These interpretations emphasize the need to cautiously interpret the RCS model when the primary grains have a low density of particles.

Thus the volume fraction, the contact distribution, and the covariance function can be seen to have important biological interpretations which can be extended further by considering the integral feeding length scale, $\mathscr{F}$. The feeding length scale $\mathscr{F}$ may be the only example of a true biological scale inasmuch as various scales reported in the literature have no demonstrated biological function: they are simply sampling scales and accordingly anthropocentric in nature. The feeding length scale sets the length scale for patch size from the perspective of the randomly placed copepod and provides a direct link with the effect of small-scale turbulence on the feeding process.

As an example, a fixed number of phytoplankton cells, 200×10^6 cells per cubic metre (i.e. 200 cells per cubic centimetre) is allocated to different Boolean patch structures to show that fixed densities of cells can represent different grazing opportunities (see table 1). The cells are allocated to 50 and 500 patches per cubic metre maintaining intra-patch densities of 400 and 800 cells per cubic centimetre. For this

PHILOSOPHICAL TRANSACTIONS OF THE ROYAL SOCIETY B BIOLOGICAL SCIENCES

Table 1. *Statistics representing an example of fixed allocations of 200×10^6 cells per cubic metre to 50 and 500 patches with 400 and 800 cells per patch*

cells per cubic metre	cells per cubic centimetre per patch	patches per cubic metre	volume of patch / cm^3	patch radius / cm	within patch NND / cm	between patch centre NND / cm	patch s.d. / cm	volume fraction (p)	Integral scale / cm
200×10^6	400	50	10000	13.365	0.0746	14.93	6.5	0.55	34
		500	1000	6.2035	0.0746	6.93	3.0	0.55	30
	800	50	5000	10.608	0.0592	14.93	5.5	0.39	18
		500	500	4.923	0.0592	6.93	2.5	0.37	15

particular example the total number of cells 200×10^6 was divided by either 50 or 500 giving the number of cells per patch: 4×10^6 or 0.4×10^6, respectively. The number of cells per patch was then divided by the patch density (400 or 800 cells per cubic centimetre) to obtain the patch volume. The patch radius was then determined directly from the volume. To obtain the covariance function it is necessary to assume some positive value for the radius variance, we let the standard derivation equal approximately one half the mean radius.

Table 1 shows that if the within-patch density is fixed, then the within-patch NND and the volume fraction is constant. On the other hand, if the number of patches per-unit volume is fixed, then only the distance between the patches remains constant. Both the volume fraction and the integral scale vary over all four cases. Note, however, that because in this example the ratios $r^3:\lambda$ are large the propensity for coalescence is also large (compare the patch NND with the patch radius).

To take a different tack the volume fraction could have been restricted to values smaller than $p = 0.1$ (cf. figure 10). The 200×10^6 cells per cubic metre could have been maintained at patch densities 50 patches per cubic metre. This means that we have all concentrations of 0.8×10^{10} cells per cubic metre or 0.8×10^4 cells per cubic centimetre within each patch a seemingly high concentration.

The constraints reflect that 'reasonable' cell densities result in large spheres, large volume fractions, and a high degree of coalescence and a complex patch structure. On the other hand, if we fix the size of the patch at a small value relative to the density of patches, we have a small volume fraction, a low degree of coalescence, a simple structure, but a seemingly high concentration of cells. It is not known which case actually obtains in nature, because feeding-scale patch structure is not generally reported.

The covariance functions based on table 1 are plotted for each of the four cases in figure 11. Note, that as pointed out in the theoretical section, the upper and lower bounds of the covariance function are the volume fraction and the volume-fraction squared, respectively. Inasmuch as the volume fractions depend only on the density of patches and their radius, and the variance and the volume of patches is held constant for 400 cells per cubic centimetre and 800 cells per cubic centimetre cases, the upper and lower bounds for each of these cases is the same. However, in both instances the many smaller patches result in a much more rapid decline in the covariance function.

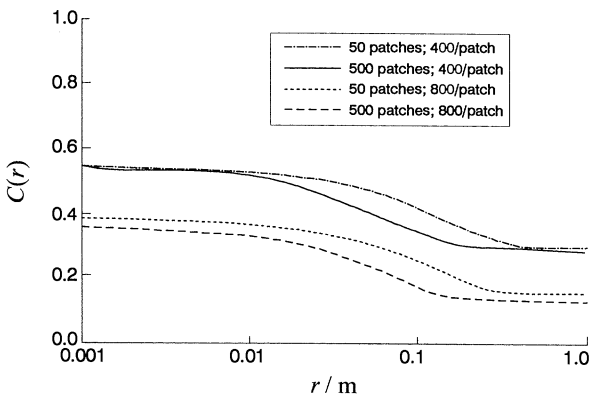

Figure 11. Covariance function as a function of distance from patch centre for the cases indicated in table 1. Note that the Kolmogorov length scale can be superimposed on the x-axis. Its position would depend upon the magnitude of ε.

The contact distribution for the four cases in table 1 is shown in figure 12. The contact distribution can be thought of in terms of the search opportunities of a grazing copepod. In this case the results are asymmetrical with those for the covariance function in the sense that there is more similarity within the number

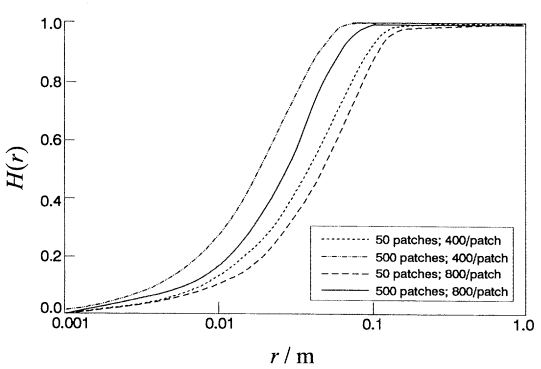

Figure 12. The 'horizon' for a copepod not in a patch searching for a patch. $H(r)$ is the probability of the nearest patch being at a distance r. Even though the overall density of phytoplankton cells is fixed, allocations to more patches result in higher values of $H(r)$. Given the particular allocation algorithm higher density patches are smaller and hence more distant.

PHILOSOPHICAL TRANSACTIONS OF THE ROYAL SOCIETY B BIOLOGICAL SCIENCES

of patches per unit volume then between the number of patches per unit volume.

Even though the overall density of phytoplankton cells is fixed, allocations to 500 rather than 50 patches per cubic metre result in higher values of $H(r)$ and hence lower values of $\bar{r}_h$. Given the particles allocation scheme, high-density patches are smaller and hence more distant.

The significance of these statistics is apparent from two points of view. From one point of view they show how fixed densities of particles can result in very different feeding conditions. From a second point of view they set the stage for demonstrating how patch structure is related to physical processes.

4. COUPLING WITH PHYSICAL PROCESSES

The effects of turbulent flow on particles relates to both the density of particles and their relative motion. The complex inter-relationships (cf. Davis *et al.* 1991; Costello *et al.* 1990; Marrasé *et al.* 1990; Sundby & Fossum 1990) depend upon (i) how the particles are distributed in the flow field; (ii) the specifics of the flow; and (iii) the swimming or other behaviour of the particle. From the point of view of the relative motion of particles, both point-process and RCS theory establish initial conditions and a metric for summarizing information on particle trajectories. In the theory of homogenous-and-isotropic turbulence, the relative uncorrelated velocity of two particles depends upon the turbulent-energy dissipation rate and the distance between the particles. For patch-structure cases, point-process theory gives the probability distribution of the distance between particles under a variety of patch models. It also gives the second-order properties of the distribution. The RCS theory gives the probability distribution of distance from outside a patch, the contact distribution; and from inside a patch, the covariance function.

The problem is now converted to a 'function-of-random-variables problem' where the probability distribution of the relative velocity of particles depends more generally upon (i) the distribution of interparticle distances in the point-process sense and (ii) or the contact distribution or the covariance function in the RCS theory sense. This sets the stage for coupling 'basin-scale' wind events (see, for example, Dickson *et al.* 1988; Rothschild & Osborn 1988; Oakey & Elliott 1982; Sundby & Fossum 1990) with microscale feeding events. Because wind events can operate over a very large area, the wind variations integrate encounter rates over a large area.

The interesting but very important nuance is that the above argument assumes that the particles are immotile: that is they are always at some physical equilibrium (apart from a Stokes-equation considerations). A comparison of the spatial geometry of motile particles with the spatial geometry of similar immotile particles then reflects a minimum bound on various energetics required by these organisms for their survival. As this bound must change with physical forcing, another critical link between ecosystem dynamics and physics is established.

From the point of view of diffusive–dispersive processes the picture seems to be not as clear because dispersive processes can either enhance or reduce the density of organisms depending upon the nature of the process and the initial distribution of organisms. We can infer that the well-known conditions for patch maintenance are such that the length-scale geometry of a patch must be greater than a function of the diffusion coefficient, and the birth and death rate of the particles in the patch, namely

$$L > \phi(\alpha), \qquad \alpha = (D/\beta - \delta)' \tag{24}$$

where L is the patch dimension, D is the diffusion coefficient associated with the patch and β and δ are birth and death rates respectively. This means that if birth and death rates do not change, but diffusion increases then the critical dimensions of the patch would need to increase. Similarly, a decrease in the diffusion constant implies that smaller patches could be maintained. Further, as birth rates increased over death rates larger patches could be maintained. This of course requires some timescale for L and the birth and death rates such that equation 24 is meaningful. It can, however, be seen immediately that all of the nuances of RCS apply to L.

Finally, the theory of RCS can be used to simplify our thinking on the turbulent flow problem. The difficulty to be overcome is that the motion of particles that are close together is coupled. The motion of particles that are distant is uncorrelated. The point at which the motion becomes decorrelated is a function of ε. We therefore establish a different type of microzone about each particle, the radius of which is a function of ε. We can then study the relatively easy problem of uncorrelated motion among particles with interparticle distances at least as great as the specified microzone radius and establish in this context biological–physical consequences of the volume fraction, the contact distribution, and the covariance function.

5. CONCLUSIONS

This paper has approached understanding community metabolism at the fundamental level of particle–particle interactions. This approach has illustrated the importance of characterizing the spatial structure of interacting particles in evaluating the significance of average densities. The statistics of stochastic geometry such as spheres of influence and coalescence are directly relatable to biological features of planktonic predator–prey systems. However, much further work needs to be done.

Setting in motion the geometric representation of particles will be a difficult task. How this might be approached can be seen by considering the distribution of particle velocity with respect to homogeneous and isotropic turbulence where patch structure is taken into account. Complexities for future consideration involve the effects of turbulent flow on particle density (e.g. diffusion) and exploring the alternative circumstances leading to increases or decreases in particle density. An additional important aspect is the motility of particles. Particles that are motile and not

PHILOSOPHICAL TRANSACTIONS OF THE ROYAL SOCIETY B BIOLOGICAL SCIENCES

in physical equilibrium have expended metabolic energy to reach or maintain their non-equilibrium point. This will affect interpretation of interparticle distances as a fabric for predator–prey interactions.

A still complex issue is how to combine species into meaningful groups for the description of community metabolism. While taxonomic (or size-based) groupings are attractive, owing to their simplicity, grouping community members by metabolic-variability characteristics may be more useful. If the goal of upper-ocean studies is to understand variability in community metabolism, then consideration of interparticle distances, however particles are classified, will lend insights into the aspects of spatial structure which both integrates and differentiates influences of physical and biological processes.

The present analysis of interparticle nutrient flux and grazing suggest that many plankters are closer spatially than generally thought. This analysis is conservative in that a static geometric approach was taken. This, however, strengthens the argument that spatial distributions are key, turbulent-flow affected factors governing nutrient flux among organisms. Both point-processes and RCS theory lends itself to studying the geometry of proximity. Point-process theory establishes the distinction between no-information random search where $\bar{r}$ is important and non-random search where r^* is important. RCS theory provides a useful statistical framework of the study of microzones and their kinetics.

Concerning grazing, the effects of different spatial distributions parameterized by the same mean prey density, can be substantial. The transition from random-particle distribution to random-patch structure in the point-process case, from both order statistics and RSOMF, quantitatively demonstrates the potential importance of non-random search patterns. This makes the speculation about the role of microplankton as chemical 'repeaters' that guide grazers to patches of larger autotrophs a fascinating issue for further modelling.

An important question involves the significance of any theoretical result. Is a one-percent or a thirty-percent change in encounter rate important? The answer depends upon the particular circumstances. It can be said, however, from the study of nonlinear population dynamics, that even the slightest change in a trophodynamic parameter (in the community matrix, for example) can result in substantial qualitative and quantitative differences in population trajectories (see also Beyer 1989).

The RCS theory lends considerable new flexibility to the study of grazing in the upper ocean. Patch structure in the context of RCS, the onset of coalescence, and effects of physical structure on feeding scales reflect components of biodynamic flux of the upper ocean. Although all of these aspects are functions of the effects of interparticle distance on trophodynamics, they relate as well to population dynamics and to community metabolism. Thus, in undertaking the particulate description of community metabolism, the modes of required measurement shift to the measurement of particle numbers, and interparticle distances establishing a yet additional role of stochastic geometry, the development of statistical requirements for the development of acoustic and optic sensors.

Discussions with D. Capone were helpful in thinking about microplankton ecology. D. S. Robson read the paper and provided helpful insights. Huaxing Li computed the covariance and contact distribution functions. Comments from D. H. Cushing, J. S. Steele and M. J. Fasham were helpful toward completing the paper.

REFERENCES

Allee, W.C., Emerson, A.E., Park, O., Park, T. & Schmidt, K.P. 1949 *Principles of animal ecology*. Philadelphia: (837 pages.) W. B. Saunders Company.

Beyer, J.E. 1989 Recruitment stability and survival-size specific theory with examples from the early life dynamics of fish. *Dana* **7**, 45–147.

Cassie, R.M. 1959 Micro-distribution of plankton. *N.Z. Jl Sci.* **2,** 398–409.

Costello, J.H., Strickler, J.R., Marrasé, C., Trager, G., Zeller, R. & Freise, A.J. 1990 Grazing in a turbulent environment: Behavioral response of a calanoid copepod, *Centropages hamatus*. *Proc. natn. Acad. Sci. U.S.A.* **87**, 1648–1652.

Davis, C.S., Flierl, G.R., Wiebe, P.H. & Franks, P.J.S. 1991 Micropatchiness, turbulence and recruitment in plankton. *J. mar. Res.* **49**, 109–151.

Dickson, R.R., Kelly, P.M., Colebrook, J.M., Wooster, W.S. & Cushing, D.H. 1988 North winds and production in the eastern North Atlantic. *J. Plank. Res.* **10**, 151–169.

Fasham, M.J.R. 1978*a* The Statistical and Mathematical Analysis of Plankton Patchiness. *Oceanogr. mar. Biol.* **16**, 43–79.

Fasham, M.J.R. 1978*b* The application of some stochastic processes to the study of plankton patchiness. In *Spatial pattern in plankton communities* (ed. J. H. Steel) (NATO Conference Series IV: Marine Sciences), pp. 131–156. New York: Plenum Press.

Gerritsen, J. & Strickler, J.R. 1977 Encounter probabilities and community structure in zooplankton: a mathematical model. *J. Fish. Res. Bd Can.* **34**, 73–82.

Goldman, J.C. 1988 Spatial and temporal discontinuities of biological processes in pelagic surface waters, In, *Toward a theory on biological-physical interactions in the world ocean* (ed. B. J. Rothschild) (NATO ASI Series C: vol. 239), pp. 273–296. Boston: Kluwer Academic Publishers.

Holling, C.S. 1965 The functional response of invertebrate predators to prey density and its role in mimicry and population regulation. *Mem. ent. Soc. Can.* **45**, 1–60.

Jackson, G.A. 1987 Physical and Chemical Properties of Aquatic Environments. In Ecology of microbial communities (ed. M. Fletcher, T. R. G. Gray & J. G. Jones), pp. 213–233. Cambridge University Press.

Jahnke, R.A. 1990 Ocean flux studies: a status report. *Rev. Geophys.* **28**(4), 381–398.

LeFèvre, J. & Frontier, S. 1988 Influence of temporal characteristics of physical phenomena on plankton dynamics as shown by North-West European marine ecosystems. In *Toward a theory on biological physical interactions in the world ocean* (ed. B. J. Rothschild) (NATO ASI Series C: vol. 239), pp. 245–272. Boston: Kluwer Academic Publishers.

Longhurst, A.R. & Harrison, W.G. 1989 The biological

PHILOSOPHICAL TRANSACTIONS OF THE ROYAL SOCIETY B BIOLOGICAL SCIENCES

pump: profiles of plankton production and consumption in the upper ocean. *Prog. Oceanogr.* **22**, 47–122.

Mann, K.H. & Lazier, J.R.N. 1991 Dynamics of marine ecosystems: biological-physical interactions in the oceans (466 pages.) Boston, Massachussetts: Blackwell Scientific Publications.

Marrasé, C., Costello, J.H., Granata, T. & Strickler, J.R. 1990 Grazing in a turbulent environment: energy dissipation, encounter rates, and efficacy of feeding currents in *Centropages hamatus*. *Proc. natn. Acad. Sci. U.S.A.* **87**, 1653–1657.

Mitchell, J.G., Okubo, A. & Fuhrman, J.A. 1985 Microzones surrounding phytoplankton form the basis for a stratified marine microbial ecosystem. *Nature, Lond.* **316**, 58–59.

Oakey, N. & Elliott, J. 1982 Dissipation within the surface mixed layer. *J. phys. Oceanogr.* 12, pp. 171–185.

Pielou, E.C. 1977 *Mathematical ecology*. New York: Wiley.

Rothschild, B.J. 1986 *Dynamics of Marine Fish Populations*, chapter 8 (*The population-dynamics process*) (pp. 218–236.) Harvard University Press.

Rothschild, B.J. 1988 Biodynamics of the sea: The ecology of high dimensionality systems. In *Toward a theory on biological-physical interactions in the world ocean* (ed. B. J. Rothschild) (NATO ASI Series C: vol. 239), pp. 527–548. Boston: Kluwer Academic Publishers.

Rothschild, B.J. 1991 Food Signal Theory: population regulation and the functional response. *J. Plank. Res.* **13**(5), 1123–1135.

Rothschild, B.J. & Osborn, T.R. 1988 Small-scale turbulence and plankton contact rates. *J. Plank. Res.* **10**(3), 465–474.

Stoyan, D., Kendall, W.S. & Mecke, J. 1987 *Stochastic geometry and its applications* (345 page.) New York: John Wiley and Sons.

Sundby, S. & Fossum, P. 1990 Feeding conditions of Arcto-norwegian cod larvae compared with the Rothschild-Osborn theory on small-scale turbulence and plankton contact rates. *J. Plank. Res.* **12**(6), 1153–1162.

Received 11 September 1991; accepted 6 December 1991

PHILOSOPHICAL TRANSACTIONS OF THE ROYAL SOCIETY B BIOLOGICAL SCIENCES